*International Journal of Advanced Research in Physical Science (IJARPS)*
*Volume 2, Issue 6, June 2015, PP 1-8*
*ISSN 2349-7874 (Print) & ISSN 2349-7882 (Online)*
*www.arcjournals.org*

# Vibrational Resonance in the Duffing Oscillator with State-Dependent Time-Delay

**C. Jeevarathinam**
School of Physics
Bharathidasan University
Tiruchirappalli-24
*jeeva@cnld.bdu.ac.in*

**S. Rajasekar**
School of Physics
Bharathidasan University
Tiruchirappalli-24
*rajasekar@cnld.bdu.ac.in*

**Abstract:** *We consider the double-well Duffing oscillator driven by a biharmonic force with frequencies $\omega$ and $\Omega$, $\Omega \gg \omega$ with three different forms of state-dependent time-delayed feedback. The forms of delay time are sigmoid, parabolic and Gaussian functions of position variable. We investigate the effect of the parameters characterizing the forms of time-delay and the strength of the feedback term on the vibrational resonance with specific emphasize on the number of resonances, the maximum value of the response amplitude and the value of the amplitude of the high-frequency ($\Omega$) component of the driving force at which resonance occurs. The influence of the three types of delay time is found to be nontrivial. Moreover, the number of resonance and the response amplitude can be controlled by the parameters characterizing the form of the delay time.*

**Keywords:** *Vibrational resonance, Duffing oscillator, state-dependent time-delay*

## 1. Introduction

Time-delayed phenomena are ubiquitous in many nonlinear dynamical systems because of a finite signal propagation time in networks, finite switching speed of amplifiers, finite reaction, memory effects and so on [1–3]. When the state of a system at time $t$ depends on the state of the system at one or more later times a time-delayed feedback is to be introduced in the mathematical modelling of the system. The feedback can be linear or nonlinear. In the nonlinear dynamics literature the influence of different types of time-delayed feedback or coupling on the dynamics of linear and nonlinear systems are reported. It has been pointed out that time-delay can be a single constant, multiple constants, integrative over a finite interval, distributive over an interval with certain specific distributions, state-dependent and even a random [4]. The effect of certain types of time-delay on bifurcations, chaos and synchronization have been investigated.

In recent years much interest has been focused on the role of time-delay on vibrational resonance. In a nonlinear system driven by a biharmonic periodic force with two frequencies $\omega$ and $\Omega$ with $\Omega \gg \omega$ the amplitude of response of the system at the low-frequency $\omega$ is found to display resonance when the amplitude of the high-frequency ($\Omega$) component of the driving force is varied. This high-frequency force induced resonance is termed as vibrational resonance [5–7]. The goal of the present paper is to report our investigation on the effect of state-dependent time-delayed (SDTD) feedback on vibrational resonance. SDTDs were appeared in the modelling of transmission channels of communication networks [8], in supply networks as a consequence of transportation of materials [9–11], in population dynamics [12] and in engine cooling systems [13].

There are some notable studies on the dynamics of systems with SDTDs. It is noteworthy to cite some of them. Stability theorems of equilibrium points [14–16] and periodic solutions [17,18] and numerical analysis of stability of equilibrium points and periodic solutions [19], predictor-feedback design [20], rapidly oscillating periodic solutions [21] of a class of equations with SDTDs have been reported. Occurrence of Hopf bifurcation with SDTDs in a weakly damped nonlinear oscillator [22] and machine-tool vibrations [23, 24] was analysed. Local and global stability analysis for linear and nonlinear systems [25] and the existence of periodic solutions in Lotka-Volterra systems [26] were studied. Position-dependent axonal conduction time-delays ranging from 0.1ms to 44ms was noticed in the mammalian neocertex [27, 28]. Synchronization in a neural network with time-delay depending on the distance between neurons was considered [29].

In the present paper, we investigate the vibrational resonance phenomenon in the Duffing oscillator with a state-dependent time-delayed feedback and driven by a biharmonic force. The equation of motion of the system is

$$\ddot{x} + d\dot{x} + \omega_0^2 x + \beta x^3 + \gamma x(t - \tau(x(t))) = f\cos\omega t + g\cos\Omega t, \tag{1}$$

where $\tau(x(t))$ is the state-dependent time-delay. We analyse the effect of sigmoid, parabolic and Gaussian functional forms of time-delay. The values of the parameters characterizing the functional forms of time-delay have a strong influence on number of resonance and the value of the response amplitude $Q$ at which resonance occurs.

## 2. Effect of Different Types of Position-Dependent Time Delay

First we consider the effect of sigmoid state-dependent time-delay.

### 2.1. Sigmoid State-Dependent Time-Delay

We consider the Duffing oscillator Eq. (1) with the time-delay

$$\tau(x(t)) = \frac{\tau_0}{1+\mathrm{e}^{px}}, \tag{2}$$

where $\tau_0$ is a positive constant and $p$ is a constant. $\tau(x)$ is a sigmoid function.

For $\Omega \gg \omega$ it is reasonable to assume the solution of Eq. (1) as $x(t) = X(t) + \psi(t, \Omega t)$ where $X$ and $\psi$ are slow motion with period $2\pi/\omega$ and fast motion with period $2\pi/\Omega$, respectively. We are interested in the response amplitude $Q$ at the low-frequency $\omega$. To compute the response amplitude $Q$ of the slow component $X$ of $x(t)$ we numerically integrate Eq. (1) using the Euler method with step size $\Delta t = 0.001$. At each time we calculate $\tau$. Since $\Delta t = 0.001$ the values of $\tau$ must be integer multiples of $\Delta t$. In order to make $\tau(x(t))$ in multiples of $\Delta t$ we write

$$\tau(x(t)) = \frac{1}{1000}\,\mathrm{Int}\left[\frac{1000\tau_0}{1+\mathrm{e}^{px}}\right], \tag{3}$$

where Int($y$) means integer part of $y$. We leave the solution corresponding to the first 1000 drive cycles of low-frequency force as a transient. Then we compute numerically the sine and cosine components $Q_S$ and $Q_C$, respectively, from the equations

$$Q_S = \frac{2}{kT}\int_0^{kT} x(t)\sin\omega t\, dt, \quad Q_C = \frac{2}{kT}\int_0^{kT} x(t)\cos\omega t\, dt, \tag{4}$$

where $T = 2\pi/\omega$ and $k = 500$. Then $Q = \sqrt{Q_S^2 + Q_C^2}\,/\,f$.

We fix the values of the parameters in (1) as $d = 0.5$, $\omega_0^2 = -1$, $\beta = 1$, $f = 0.1$, $\omega = 1$, $\Omega = 10$ and $\tau_0 = 1$. When $g$ is varied for $\gamma = 0$ there are two resonances with same response amplitude $Q$. The resonances occur at g = 54 and 115. We denote the values of g at which first and second resonances occur as $g_{\mathrm{VR}}^{(1)}$ and $g_{\mathrm{VR}}^{(2)}$, respectively. Figure 1 illustrates the variation of $Q$ with the control parameters $\gamma$ and g for four different values of $p$. We can clearly notice the effect of $\gamma$ and $p$ on the resonance and on the value of $Q$. For a fixed value of $p$ the values of g at which resonances occur shift towards the origin, that is, $g_{\mathrm{VR}}$ is decreased. $g_{\mathrm{VR}}^{(1)}$ Decreases much faster than $g_{\mathrm{VR}}^{(2)}$ with increase in the value of $\gamma$. However, $Q$ at $g_{\mathrm{VR}}^{(1)}$ decreases with $\gamma$ whereas its value at $g_{\mathrm{VR}}^{(2)}$ increases with increase in $\gamma$. Figure 2 depicts the nontrivial variation of $Q$ with the parameter $p$ for $\tau_0 = 1$ and $\gamma = 0.4$ and for two fixed values of g. For $|p| \gg 1$, $Q(p) \approx Q(-p)$. With respect to $p$, the response amplitude $Q$ is strictly not symmetric about $p = 0$. The choice $p = 0$ gives $\tau = \tau_0/2$. In this case time-delay is a constant. In Fig. 2 for g = 54, $Q(p = 0) < Q(p \neq 0)$ while for g = 115, $Q(p = 0) > Q(p \neq 0)$ for a wide range of values of $p$.

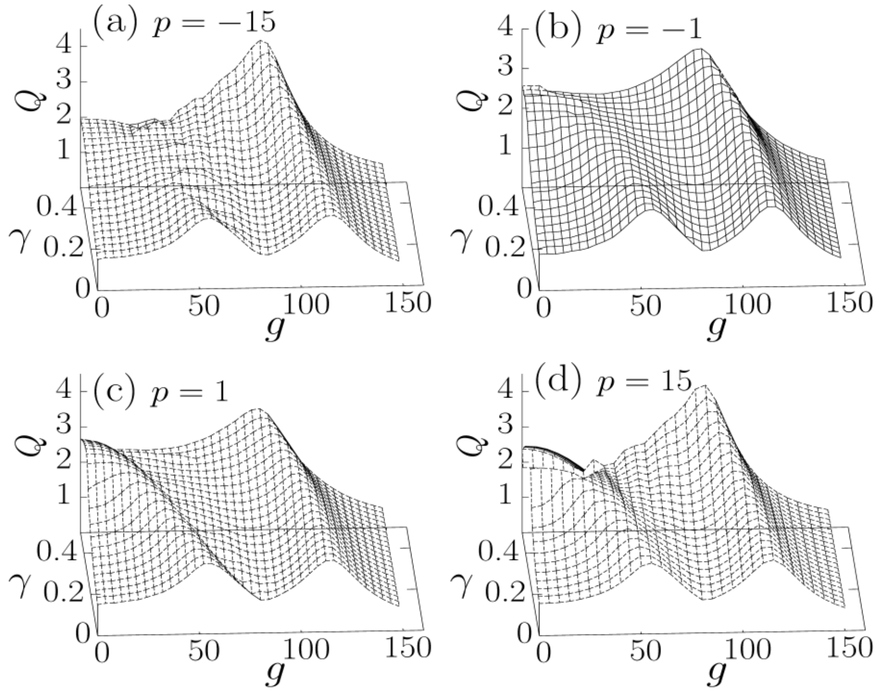


**Fig1.** *Dependence of Q on the parameters γ and g for four values of p with sigmoid function type delay time* $\tau$ *given by Eq. (2). The values of the parameters are d = 0.5,* $\omega_0^2 = -1$*, β = 1, f = 0.1, ω = 1, Ω = 10 and* $\tau_0 = 1$*.*

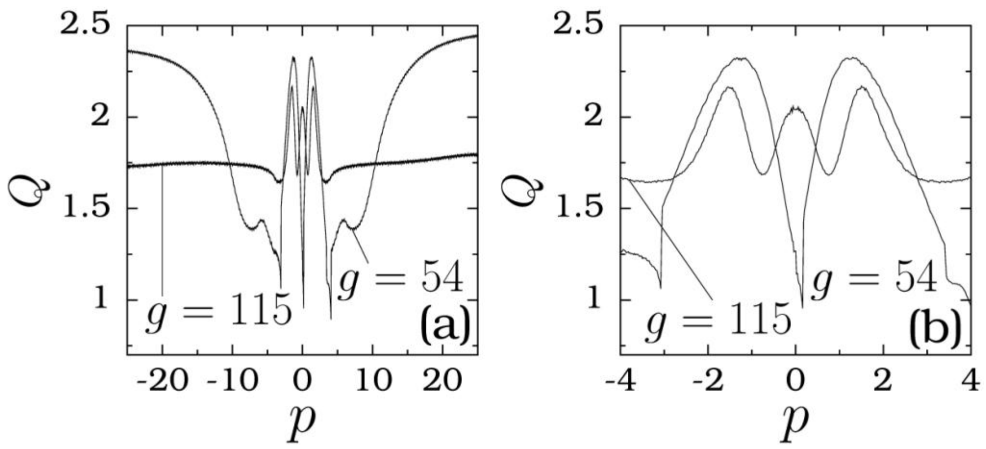


**Fig2.** *(a) Q versus p for g = 54 and 115 at which resonance occurs when γ = 0. Here γ = 0.4 and* $\tau_0 = 1$*. The time-delay* $\tau(x)$ *is given by Eq. (2). (b) Magnification of subplot (a) in the interval* $p \in [-4, 4]$*.*

In Fig. 3 we plot $x(t)$ versus $t$ for four values of g. We fixed $\tau_0 = 1$, $p = -1$ and $\gamma = 0.2$. The left (right)-panel shows the result for an initial condition chosen in the neighbourhood of the left (right)-well minimum. For small values of g there are two orbits - one is confined to $x < 0$ while another is confined to $x > 0$. The values of $Q$ for these two orbits are the same. The value of $Q$ for the orbits shown in Figs. 3a and 3e for g = 10 is 1.49. In this figure only the orbit lying in the interval $x < 0$ is shown. $Q$ increases with increase g and at g = 42, $Q$ becomes a maximum with the value 2.3. At resonance also there are two different orbits confined to $x < 0$ and $x > 0$, respectively. This is shown in Figs. 3b and 3f. There is no cross-well motion. That is, cross-well motion is not a precursor for resonance. As the value of g is further increased from $g_{\mathrm{VR}}^{(1)} = 42$ the trajectories begin to visit the regions $x < 0$ and $x > 0$. However, the two co-existing orbits are not symmetric about origin. This is evident from Figs. 3c and 3g where g = 82. The value of $Q$ for these two orbits is 1.56. The value of $Q$ decreases with increase in g beyond $g_{\mathrm{VR}}^{(1)}$.

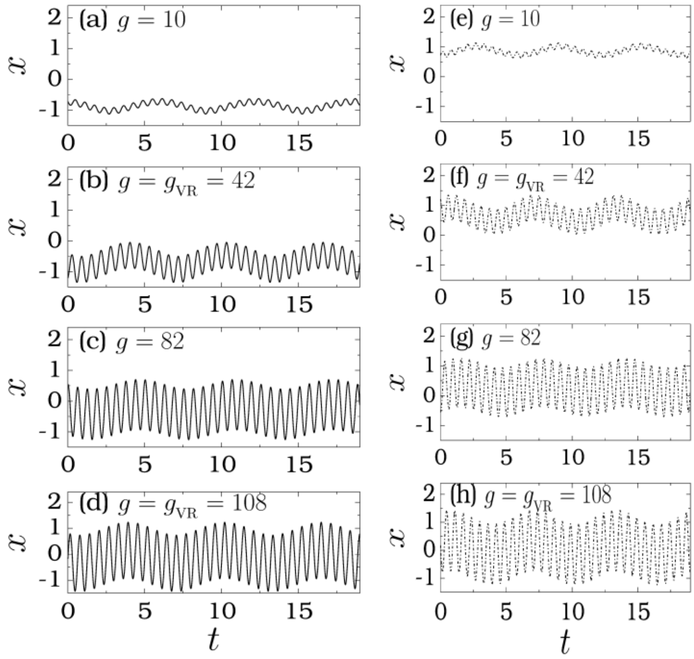

**Fig3.** *Time series plot for four values of g for the system (1) with delay time being of the form of sigmoid function Eq. (2). Here $\tau_0$ = 1, p = −1 and γ = 0.2. For the subplots (a)-(d) and (e)-(h) the initial condition is chosen in the neighbourhood of the left-well minimum and the right-well minimum, respectively.*

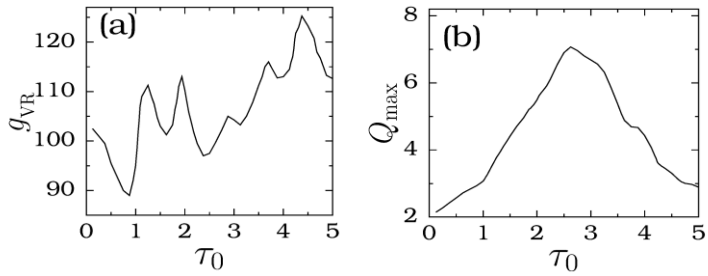

**Fig4.** (a) $g_{\mathrm{VR}}$ versus $\tau_0$ and $Q_{\max}$ versus $\tau_0$ for the system (1) with sigmoid function type of time delay. The values of the parameters in the time-delayed feedback term are fixed as $\gamma = 0.4$ and $p = -1$.

At a value of g the response amplitude $Q$ becomes minimum and then $Q$ increases with increase in g. A second resonance occurs at g = $g_{\mathrm{VR}}^{(2)}$ = 108. The corresponding value of $Q$ is 2.48. We note that $Q$ at $g_{\mathrm{VR}}^{(1)}$ and $g_{\mathrm{VR}}^{(2)}$ are not the same. Figures 3d and 3h show the orbits for g = 108. By looking at the trajectories or phase portrait for a range of values of g it is not possible to determine the values of g at which resonance takes place.

For a range of fixed values of $\tau_0$ the control parameter g is varied from zero and its critical values

$g_{\mathrm{VR}}$ at which resonance occur and the corresponding value of $Q$ are numerically computed. When there are two resonances one at g = $g_{\mathrm{VR}}^{(1)}$ and another at $g_{\mathrm{VR}}^{(2)}$ with $g_{\mathrm{VR}}^{(1)} \neq g_{\mathrm{VR}}^{(2)}$ we choose the critical value as the one for which $Q$ is larger. Figure 4a shows the variation of $g_{\mathrm{VR}}$ with $\tau_0$ for $\tau_0 \in [0, 5]$. $g_{\mathrm{VR}}$ oscillates with $\tau_0$. In Fig. 4b $Q_{\max}$ (the value of $Q$ at g = $g_{\mathrm{VR}}$) increases with $\tau_0$, reaches a maximum at a value of $\tau_0$ and then decreases. That is, $g_{\mathrm{VR}}$ and the value of $Q$ can be controlled by the parameter $\tau_0$.

## 3. Parabolic State-Dependent Time-Delay

Next, we consider the system (1) with the time-delay being of the form $\tau(x(t)) = \tau_0(1 + px^2)$. where $\tau$ $(x(t))$ is quadratic in $x$. In order to make $\tau \geq 0$ we choose $p > 0$ and $\tau_0 > 0$.

Figures 5a and 5b show the response amplitude profile, $Q$ versus g, for a range of values of γ for $\tau_0$ = 0.6 and for $p$ = 0.2 and 0.9. These two figures can be compared with Fig. 1 where the time-delay is a sigmoid function type. For a range of fixed values of γ and $p$ two resonances occur when the parameter g is varied. Both $g_{\mathrm{VR}}^{(1)}$ and $g_{\mathrm{VR}}^{(2)}$ move towards origin. In Fig. 5a ($p$ = 0.2) for γ< 0.5 there are two resonances, only one resonance for 0.5 < γ < 0.95 while for γ > 0.95 there is no resonance when g is varied. Further, for γ > 1, $Q$(g) ≈0. Similar results are found for other values of $p$. However, for example, in Fig. 5b corresponding to $p$ = 0.9, we observe a number of resonance peaks for each fixed value of γ. The second resonance peak is the dominant resonance for a range of values of g. The amplitude of the resonance peaks decays with increase in g.

Figures 5c and 5d depict the effect of $\tau_0$ and $p$, respectively, on the resonance curve for fixed values of other parameters. Here again a sequence of resonance peaks occur when g is varied.

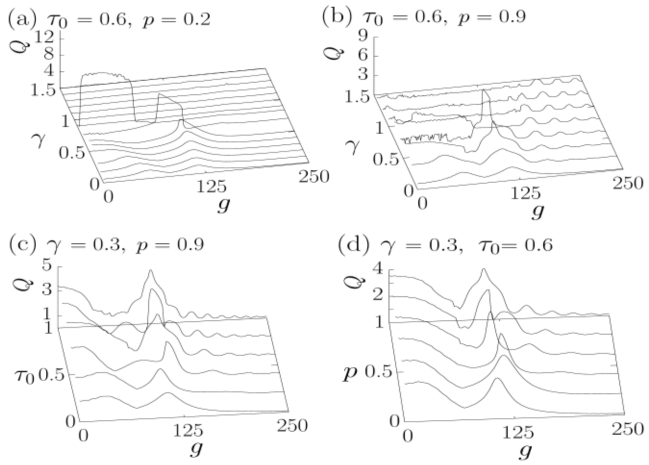


**Fig5.** *The results for the system (1) with parabolic type state-dependent delay. (a)-(b) γ versus g versus Q for p = 0.2 (a) and p = 0.9 (b) with* $\tau_0$ *= 0.6. (c)* $\tau_0$ *versus g versus Q for γ= 0.3 and p = 0.9. (d) p versus g versus Q for γ = 0.3 and* $\tau_0$ *= 0.6.*

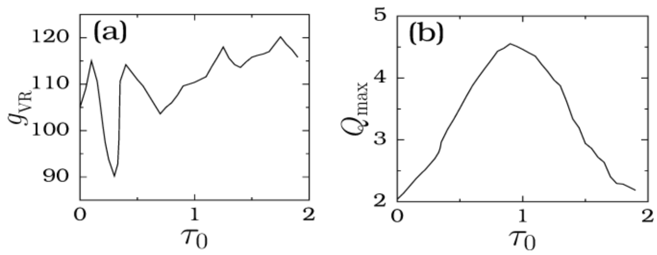


**Fig6.** *Variation of (a)* $g_{\mathrm{VR}}$ *and (b) Qmax the value of Q at g =* $g_{\mathrm{VR}}$ *with the parameter* $\tau_0$ *for the system (1) with the delay time being given by Eq. (5). Here p = 0.9 and γ = 0.3.*

The number of resonance peaks increases with increase in the value of $\tau_0$ and $p$. In Fig. 5 we find that the range of time-delay increases with increase in $\tau_0$ and $p$.

For a relatively small range of delay time ($p$ and $\tau_0$ are small) the response amplitude profile does not exhibit multiple peaks. Damped oscillation of $Q$ occurs when the delay time interval is sufficiently large ($p$ and $\tau_0$ are large). The multi-resonance peaks are not realized when the time-delay is a sigmoid function. In Fig. 6 we plot the $g_{\mathrm{VR}}$ (the value of g at which $Q$ is the largest) and the corresponding value of $Q$, $Q_{\mathrm{max}}$ as a function of $\tau_0$. The variation of these two quantities in the case of parabolic time-delay is similar to the case of sigmoid function time-delay. Though $g_{\mathrm{VR}}$ oscillates with $\tau_0$, the value of $Q_{\mathrm{max}}$ increases with increase in $\tau_0$ from a small value, reaches a maximum at a value of $\tau_0$ and then decreases. The value of $Q_{\mathrm{max}}$ can be controlled by $\tau_0$.

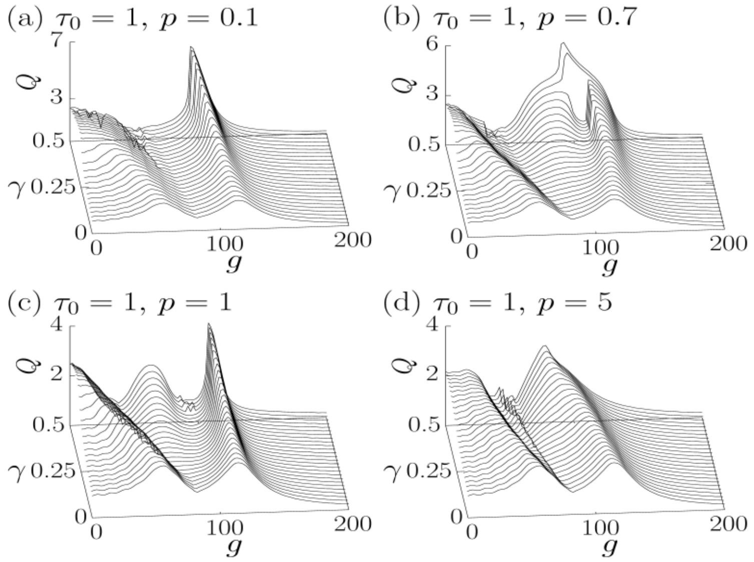


**Fig7.** *Q versus γ versus g for the system (1) with the time-delay* $\tau(x(t)) = \tau_0 e^{-px^2}$ , $\tau_0$ *= 1 and for four fixed values of p.*

## 4. Gaussian Delay-Time

In the previous two subsections we considered sigmoid function and parabolic type delay- time. In the sigmoid function case (refer Eq. (2)) depending upon the value of *p* the delay time $\tau(x(t)) \approx 0$ either for $x \gg 0$ or for $x \ll 0$. In this subsection we consider a form of $\tau$ which decays to 0 as $|x|$ increases from a small value. An example is the Gaussian form of $\tau$ given by $\tau(x(t)) = \tau_0 e^{-px^2}$.

Figure 7 presents the effect of the parameters γ, *p* and g on the response amplitude for $\tau_0 = 1$. For small values of *p* the system exhibits double resonance when g is varied for a range of fixed values of γ. For γ greater than a critical value only one resonance occurs. This is shown in Fig. 7a. Three resonances occur for a range of fixed values of *p* and γ. We can clearly notice three resonances in Figs. 7b and 7c. In Fig. 7d for *p* = 5, a large value of *p*, the middle resonance is weak. Here also the values of g at which resonances occur move towards origin as the value of γ increases. The rate of changes of the values of g at which second and third resonances occur is much slower than the first resonance. The values of Q at the resonances increase with increase in the value of γ.

Figure 8 shows the variation of $g_{\rm VR}$ (the value of g at which the value of *Q* is the largest) and the corresponding *Q*, $Q_{\max}$, with the parameter $\tau_0$ for γ = 0.3 and *p* = 0.1. $g_{\rm VR}$ oscillates with $\tau_0$. The oscillation is much smoother than for the cases of sigmoid function and parabolic type time-delay (Figs. 4a and 6a). Here again $Q_{\max}$ increases with increase in the value of $\tau$, reaches a maximum at a value of $\tau_0$ and then decreases.

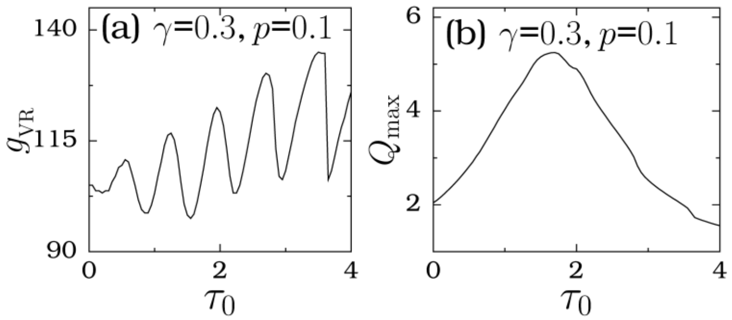


**Fig8.** *(a)* $g_{\rm VR}$ *versus* $\tau_0$ *and (b)* $Q_{\max}$ *(g =* $g_{\rm VR}$ *) versus* $\tau_0$ *for the system (1) with the Gaussian type position dependent time-delay.*

## 5. Conclusions

In this present paper we reported our study on the vibrational resonance in the double- well Duffing oscillator system with position-dependent time-delayed feedback. We considered three forms of the delay time: sigmoid function, parabolic function and Gaussian function of position variable. In the absence of time-delay, for the parametric choices used in our study two resonances with same response amplitude at resonance is found. Nontrivial effects are realized in the presence of the position-dependent time-delayed feedback. An interesting feature of $\tau = \tau_0(1 + px^2)$ is the occurrence of multiple vibrational resonance for a range of values of $p$ and the feedback strength γ. For a range of values of the control parameters of the three forms of time-delay $Q(g, \tau) > Q(\tau = 0)$. In the three forms of the time-delay the maximum value of the response amplitude $Q$ is found to increase with the value of $\tau_0$, reaches a maximum at a value of $\tau_0$ and then decreases with further increase in the value of $\tau_0$. $Q$ can be controlled by means of the parameters characterizing the form of distributive time-delay and the strength of the feedback term.

## Acknowledgments

CJ expresses his gratitude to University Grants Commission (U.G.C.), India for financial support in the form of U.G.C. meritorious fellowship.

## References

[1] J. Chiasson and J.J. Loiseau, *Applications of Time-Delay Systems*. Berlin: Springer, 2007.

[2] J.J. Loiseau, W. Michiels, S.I. Niculescu, and R. Sipahi, *Topics in Time Delay Systems: Analysis, Algorithms, and Control*. Berlin: Springer, 2009.

[3] F.M Atay, *Complex Time-Delay Systems: Theory and Applications*. Berlin: Springer, 2010.

[4] M. Lakshmanan and D.V. Senthilkumar, *Dynamics of Nonlinear Time-Delay Systems*. Berlin: Springer, 2010.

[5] P.S. Landa and P.V.E. McClintock, Vibrational resonance, J. Phys. A: Math. Gen. 33, L433 (2000).

[6] M. Gittermann, A bistable oscillator driven by two periodic fields, *J. Phys. A*, 34, L355 (2001).

[7] I.I. Blekhman and P.S. Landa, Conjugate resonances and bifurcations in nonlinear systems under biharmonic excitation, Int. J. Non-Linear Mech. 39, 421 (2004).

[8] E. Witrant, C.C. de-Wit, D. Georges and M. Alamir, Remote stabilization via communication networks with a distributed control law, IEEE Trans. Autom. Control 52, 1480 (2007).

[9] R. Sipahi, S. Lammer, D. Helbing and S.I. Niculescu, On stability problems of supply networks constrained with transport delay, J. Dynamic Systems, Measurement and Control 131, 021005 (2009).

[10] R. Sipahi, F.M. Atay and S.I. Niculescu, Stability of traffic flow behavior with distributed delays modeling the memory effects of the drivers, SIAM J. Appl. Math. 68, 738 (2007).

[11] J.D. Sterman, *Business Dynamics: Systems Thinking and Modeling for a Complex World*. New York: McGraw-Hill, 2000.

[12] J.M. Mahaffy, J. Belair and M.C. MacKey, Hematopoietic model with moving boundary condition and state dependent delay: Applications in erythropoiesis, J. Theor. Biol. 190, 135 (1998).

[13] M. Hansen, J. Stoustrup and J.D. Bendtsen, Modeling of nonlinear marine cooling systems with closed circuit flow, 18th IFAC World Congress (2011).

[14] K.L. Cooke and W. Huang, On the problem of linearization for state-dependent delay differential equations, Proc. Am. Math. Soc. 124, 1417 (1996).

[15] F. Hartung and J. Turi, *Dynamical systems and Delay Differential Equations*. Kennesaw: Georgia, 2000.

[16] F. Hartung and J. Turi, Linearized stability in functional differential equations with state-dependent delays, Proceedings of the Conference on Dynamical systems and differential equations, Kennesaw: Georgia, 2001.

[17] F. Hartung, Linearized stability in periodic functional differential equations with state-dependent delays, J. Comp. App. Maths. 174, 201 (2005).

[18] H. Walther, A periodic solution of a differential equations with state dependent-delay, J. Diff. Eqs. 244, 1910 (2008).

[19] T. Luzyanina, K. Engelborghs and D. Roose, Numerical bifurcation analysis of differential equations with state-dependent delay, Int. J. Bifur. Chaos 11, 737 (2001).

[20] N.B. Liberis, M. Jankovic and M. Krstic, Compensation of state-dependent state delay for nonlinear systems, Systems and Controls Letters 61, 849 (2012).

[21] B.B. Kennedy, A state-dependent delay equation with negative feedback and "mildly unstable" rapidly oscillating periodic solutions, Disc. Cont. Dyn. Sys. Series B 18, 1633 (2013).

[22] J.I. Mitchell and T.W. Carr, Effect of state-dependent delay on a weakly damped nonlinear oscillator, Phys. Rev. E 83, 046110 (2011).

[23] A. Demir, A. Hasanov and N. Sri Namachchivaya, Delay equations with fluctuating delay related to the regenerative chatter, Int. J. Non-Linear Mech. 41, 464 (2006).

[24] T. Insperger, D.A.W. Barton and G. Stepan, Criticality of Hopf bifurcation in state-dependent delay model of turning processes, Int. J. Non-Linear Mech. 43, 140 (2008).

[25] N. Bekiaris-Liberis and M. Krstic, Compensation of state-dependent input delay for nonlinear systems, IEEE Trans. Auto. Cont. 58, 275 (2013).

[26] Y. Li and C. Wang, Positive almost periodic solutions for state-dependent delay Lotka-Volterra competition systems, Elect. J. Diff. Eqs. 91, 1 (2012).

[27] H.A. Swadlow, Efferent neurons and suspected interneurons in binocular visual cortex of the awake rabbit: receptive fields and binocular properties, J. Neurophysiol. 59, 1162 (1988).

[28] H.A. Swadlow, Monitoring the excitability of neocortical efferent neurons to direct activation by extracellular current pulses, J. Neurophysiol. 68, 605 (1992).

[29] G. Tang, K. Xu and L. Jiang, Synchronization in a chaotic neural network with time delaydepending on the spatial distance between neurons, Phys. Rev. E 84, 046207 (2011).

## AUTHORS' BIOGRAPHY

**Mr. C. Jeevarathinam (Ph.D.)** is a research scholar in the School of Physics, Bharathidasan University, Tiruchirappalli. He received his Master of Science from Bharathidasan University. His research interest is on vibrational resonance in time-delayed nonlinear single systems and coupled systems. He published four papers in peer reviewed international journals.

**Dr. S. Rajasekar** is a Professor of Physics in Bharathidasan University, Tiruchirappalli. He Published 85 papers in internationally reported Journals. He is a co-author of three text books in the field of Nonlinear Dynamics (published by Springer, 2003) and Quantum Mechanics (published by CRC press, 2015). His recent research focuses on nonlinear dynamics with a special emphasis on nonlinear resonances.